

Quantitative and qualitative analysis of neuroinflammation by beta amyloid1-42 toxin after treatment with resveratrol-loaded nanoparticles

Análise quantitativa e qualitativa da neuroinflamação pela toxina beta amiloide1-42 após tratamento com nanopartículas de resveratrol

Mariane Maria Silveira Vieira de Lima¹ , Maria Elvira Ribeiro Cordeiro¹ , Flávio Klinpovous Kerppers¹ , Ketlin Braghola¹ , Luiza Ferreira Cunha¹ , Maiara Fonseca¹ , Tatiane Budniak Mazur¹ , Christiane Schneider Machado¹ , Rubiana Mara Mainardes¹ , Afonso Shiguemi Inoue Salgado¹ , André Alexandre Pezzini² , Ana Carolina Dorigoni Bini¹ , Ivo Ilvan Kerppers¹ 

ABSTRACT

Background: This study evaluated the effects of zein nanoparticles with resveratrol on neuroinflammation caused by Alzheimer's disease. **Method:** The sample consisted of 30 animals divided into control (C), positive control (CP), white nanoparticles (NB), resveratrol nanoparticles (NR) and resveratrol (R) groups. The animals received 10 mg/kg of resveratrol or nanoparticles according to the group, daily, for 15 days, oral administration. Afterward, they were submitted to immunohistochemical (IHC) analyses. **Results:** the IHC showed that there was no change in the morphological brain composition in the NR and C groups. Conversely, in the CP, NB, and R groups, changes in the deposition of Anti Tau were observed. The NR group showed a normal projection of taurine in the axon, which was not presented in the same way in the other groups. The CD68 marker showed no microglial activation in the R and C groups. Quantitative analyses of Anti Beta-Amyloid in the NR group showed a statistical difference compared to the CP, NB, and R groups, whereas the Anti Tau analysis showed a significant difference between the CP and NR groups. The CD68 marker showed a significant difference between the C and NR groups. The analysis of cytokines showed a significant difference in TNF- α between the C and CP groups, C and NB groups, CP and NR groups, and NB and NR groups. IL-6 and InF- δ showed no significant difference between all groups. IL-10 showed significant differences between the C and NR groups, C and R groups, and CP and NR groups. **Conclusion:** NR prevented the evolution of neuroinflammation.

Keywords: Nanoparticles, Resveratrol, Alzheimer's

RESUMO

Introdução: Este estudo avaliou os efeitos das nanopartículas de zeína com resveratrol na neuroinflamação causada pela doença de Alzheimer. **Método:** A amostra consistiu em 30 animais divididos em grupos de controle (C), controle positivo (CP), nanopartículas brancas (NB), nanopartículas de resveratrol (NR) e resveratrol (R). Os animais receberam 10 mg/kg de resveratrol ou nanopartículas de acordo com o grupo, diariamente, por 15 dias, por via oral. Em seguida, foram submetidos a análises imuno-histoquímicas (IHC). **Resultados:** A IHC mostrou que não houve alteração na composição morfológica do cérebro nos grupos NR e C. Por outro lado, nos grupos CP, NB e R, foram observadas alterações na deposição de Anti Tau. O grupo NR mostrou uma projeção normal de taurina no axônio, que não se apresentou da mesma forma nos outros grupos. O marcador CD68 não mostrou ativação microglial nos grupos R e C. As análises quantitativas do antibeta-amiloide no grupo NR mostraram uma diferença estatística quando comparadas aos grupos CP, NB e R, enquanto a análise do antitau mostrou uma diferença significativa entre os grupos CP e NR. O marcador CD68 mostrou uma diferença significativa entre os grupos C e NR. A análise das citocinas mostrou uma diferença significativa no TNF- α entre os grupos C e CP, C e NB, CP e NR, e NB e NR. IL-6 e InF- δ não apresentaram diferença significativa entre todos os grupos. A IL-10 apresentou diferenças significativas entre os grupos C e NR, C e R, e CP e NR. **Conclusão:** A NR impediu a evolução da neuroinflamação.

Palavras-chave: Nanopartículas, Resveratrol, Alzheimer

¹ Mid-West State University,(PR), Brazil

² State University of West Paraná, Cascavel, (PR), Brazil.



INTRODUCTION

Neuroinflammation is reported in several observational and epidemiological studies to be the pathophysiology of Alzheimer's Disease (AD). Brain inflammation has several harmful effects that can be seen in the acute phase when inflammation is a well-established defense mechanism against infectious processes, injuries, and toxins. When the chronic inflammatory process is found, it is attributed to the activation of microglia and the release of cytokines that are found in AD¹.

AD was discovered and studied by the German psychiatrist Alois Alzheimer in 1906 and predicted to be a major cause of dementia. Other reported symptoms included failure in recent memory, paranoia, behavioral and language problems, and the presence of an atrophic brain that showed signs of β -amyloid protein (A β) deposition and neurofibrillary tangles of tau protein, characterizing senile plaques². This disease is currently linked to environmental and genetic factors³.

AD can also be associated, in rare cases, with chromosome 21 trisomy and can manifest at a younger age, in these cases around 30 years old⁴. In addition to being a disease directly linked to neurodegeneration and decreased cognition, other manifestations, such as language difficulties, memory loss, particularities in facial and name recognition, emotional instability, loss of judgment, and perceived personality changes are observed⁴.

Thus, over the past few years, AD has been investigated as a neurodegenerative dysfunction, leading to a more causal picture of dementia in the elderly population. AD causes progressive changes in brain tissue, causing loss of synapses, injury, and neuronal death in which the hippocampus is the first area to be injured⁵.

The preventive and curative treatments for this disease can increase the chances of longer life expectancy in the affected population. According to the clinical protocol and therapeutic guidelines for Alzheimer's Disease of the Brazilian Ministry of Health, an assessment with laboratory tests, imaging tests, scales, and questionnaires can evaluate signs and symptoms that lead to treatment that must be multidisciplinary. The goal of drug treatment is to provide the stabilization of

impairment over cognitive capabilities, daily activities, and behavior, reducing adverse effects⁶.

The Brazilian Unified Health System (SUS) guarantees access to medicines as part of an adequate health policy; the commitment to an adequate and free supply of medicines, including those with high cost, and the Exceptional Medicines Program includes provisions for the population affected by AD⁷.

The use of drugs with multifunctional actions correlated with biological activities in AD is seen as a viable approach to an ideal solution in the pathogenesis of the disease⁸.

Resveratrol is one of these drugs that have been investigated for the prevention and treatment of AD. It occurs in two isomeric forms - *trans*-resveratrol and *cis*-resveratrol - with dihydro-resveratrol being a metabolite of *cis* and *trans*-resveratrol with different molecular weights. The predominant and bioactive form that exhibits a broad pharmacological spectrum is *trans*-resveratrol, which has multiple functions, including reducing A β , scavenging free radicals, and inhibiting the activities of fibrillar aggregation. In addition, this polyphenol, which occurs naturally in grapes and red wine, promotes benefits against neurodegeneration due to its anti-inflammatory and antioxidant characteristics⁹.

This study evaluated the effects of zein/chitosan nanoparticles containing resveratrol in an experimental model of neuroinflammation. The effect of resveratrol and resveratrol-loaded nanoparticles on the deposition of β -amyloid was evaluated. The immunohistochemistry quantitative analyses of anti- β -amyloid, anti-Tau, and CD68 induction by β -amyloid1-42 were performed. The evaluation of pro-inflammatory (IL-6, TnF- α and InF- δ) and anti-inflammatory cytokines (IL-10) was conducted through flow cytometry in the neuroinflammation process induced by the β -amyloid toxin.

MATERIAL AND METHODS

Materials

Resveratrol was purchased from VicoFarma (Guarapuava, Brazil). Chitosan low molecular

weight (50,000-190,000 Da) (75-85% deacetylated), sodium caseinate, zein (99%) were purchased from Sigma-Aldrich (Missouri, USA). Absolute ethanol and dibasic sodium phosphate were purchased from Biotec (Lages, Brazil).

Sample

The sample contained 30 *Rattus norvegicus* Wistar strain males weighing 200-250 grams. Four animals were kept in each cage made of unbreakable and washable acrylic. All animals received feed and water *ad libitum* and were kept in a room under a 12-hour light/dark cycle (from 7 am to 7 pm) and a controlled temperature of 23 ± 1 °C. The experiment was approved by each of the Ethics Committee on the Use of Animals (CEUA) of Universidade Estadual do Centro-Oeste under protocol number 031/2019.

Experimental group

The animals were divided into five groups:

Control group (C): Consisting of 6 animals used for the evaluation of normal tissues.

Positive control group (CP): Consisting of 6 animals with lesions in the CA1 area caused by Beta Amyloid1-42 and without treatment; euthanasia and material collection occurred on the thirtieth day after injury.

Experimental group - White Nanoparticle (NB): Consisting of 6 animals with a lesion in the CA1 area by Beta Amyloid1-42 and treated with 50 mg/kg of White Nanoparticles dissolved in 0.9% saline by gavage for 15 days; euthanasia and material collection occurred on the thirtieth day after injury.

Experimental group - Resveratrol (R): Consisting of 6 animals with lesions in the CA1 area by Beta Amyloid1-42 and treated with 50 mg/kg of resveratrol dissolved in 0.9% saline by gavage for 15 days; euthanasia and material

collection occurred on the thirtieth day after injury.

Experimental group - Resveratrol Nanoparticles (NR): Consisting of 6 animals with lesions in the CA1 area by Beta Amyloid1-42 and treated with resveratrol nanoparticles at a concentration of 50 mg/kg, dissolved in 0.9% saline by gavage for 15 days; euthanasia and material collection occurred on the thirtieth day after injury.

Preparation A β 1-42

One milligram of β -amyloid peptide (Sigma-Aldrich) was dissolved in filtered Milli-Q water (0.2 μ M) and stored at -20 °C as the stock solution. Aliquots of the stock solution were thawed and kept at 37 °C for 72 hours to obtain the peptide in its fibrillated state³.

Preparation of resveratrol-loaded zein/chitosan nanoparticles

Zein nanoparticles were obtained by the liquid-liquid dispersion method described by Zhong and Jim¹⁰. Briefly, zein and resveratrol (6:1, w/w) were dissolved in 3 ml of an ethanol/water mixture (85:15, v/v) and kept under magnetic stirring (600 rpm) at room temperature for 1 h. The nanoparticles were produced by the dropwise addition of the ethanolic phase in an aqueous phase containing 2% sodium caseinate used as a stabilizer.

The mixture was kept under agitation (600 rpm) for 2 h. Subsequently, the nanoparticles were ultracentrifuged at 25151g and 25 °C for 20 min (Z36HK, HermleWehingen, BH, Germany). The supernatant was reserved for the quantitative analysis of unencapsulated resveratrol, according to the HPLC methodology of Pauluk et al.¹¹. The precipitate was resuspended in 1 mL of 0.25% chitosan solution and transferred to a shaking incubator for 1 h at 200 rpm and room temperature. The nanoparticle dispersion was ultracentrifuged for 20 min at 25 °C and 25151g, and the resulting precipitate was suspended in

water. Unloaded nanoparticles were prepared as described above, except for the addition of resveratrol.

The mean diameter and polydispersion index (PDI) of the nanoparticles were determined by the dynamic light scattering (DLS) technique (BIC 90 Plus, Brookhaven Instruments Corp., Holtsville, NY, USA). The nanoparticles were dispersed in ultrapure water and placed in a cuvette for analysis. All measurements were performed with a scattering angle of 90° at 25 °C and a laser wavelength of 659 nm.

For zeta potential determination, samples were diluted in 1 mM KCl solution and placed in an electrophoretic cell at 25 °C under a potential of ± 150 mV (ZetaSizer ZS, Malvern, UK). Measurements were taken in triplicate and expressed as mean \pm standard deviation.

Experimental surgery

The animals were anesthetized intraperitoneally with a solution of 80 mg/kg of Ketamine Hydrochloride (Ketamine, 10 ml bottle) and 15 mg/kg of Xylazine Hydrochloride (Dopaser, 10 ml bottle) and taken to a stereotaxic apparatus (David Kopf, USA) where their heads were fixed by the temporal rock and upper incisors. They were positioned according to the AP coordinates of -3.0 mm, ML = ± 1.6 mm and -1.6 mm, and DV = 3.0 mm, and lateral-lateral inclination = 0°, respectively, and taking the bregma as the reference, with the lambdoid and bregmatic sutures in the same horizontal plane.

The Beta-Amyloid toxin 1-42 (Sigma-Aldrich) was injected in the volume of 4 μ L in the hippocampal region of CA1 for 10 minutes.

After induction with the beta-Amyloid toxin, the animals rested for 30 days to allow inflammatory and neurodegenerative processes of the hippocampal neurons to occur.

Post-surgical analgesia

Tramadol hydrochloride was used at 10 mg/kg, every 12 hours orally and for seven days for postsurgical analgesia.

Treatment

All groups received the treatment by gavage of 0.5 ml with 10 mg of R and RN, and the UN group received empty particles for 15 days and after fasting for 12 hours overnight. The oral application was carefully performed always at the same time in the morning. After this process, the animals fasted for four hours, with water intake returning to normal feeding thereafter.

Euthanasia

The animals were anesthetized with 80 mg/kg of Ketamine and 15 mg/kg of Xylazine. After checking the anesthetic status, they received 175 mg/kg of Pentobarbital intraperitoneally.

Decapitation

Decapitation and subsequent removal of the brain were performed after euthanasia; the lateral ventricular region and hippocampus were placed in 15% formalin, maintained for seven days, and taken to the pathology laboratory.

Immunohistochemical analysis

Slides were produced as described for the histological analysis; however, containing two sections per slide per experimental group. Thermal dewaxing was carried out for 16 hours in an oven at 60 °C. Subsequently, chemical dewaxing was performed utilizing two immersion baths in Xylol P, for 10' each bath, and an immersion bath in 70° alcohol for another 10'. After one water bath, the slides were immersed in a sodium citrate solution in a closed container and placed in a water bath for 30' for antigen recovery.

Field marking was performed as described by Panis *et al.*¹²; the sections were delimited with a Dako Pen® hydrophobic pen and the endogenous peroxidase was blocked in a 10% hydrogen peroxide solution for 30 minutes, followed by nonspecific binding blocking by incubation in 0.1% fetal serum for 1 hour.

Subsequently, the sections were incubated with the primary antibodies (Santa Cruz Biotech), Anti Amyloid Beta (1: 300), Anti CD68, and Anti-Tau (1: 300) in a humid chamber at 4 °C for 2 hours. After incubation, the slides were subjected to 3 baths (5 minutes each) in PBS, incubated with the secondary antibody, and kept for 15 minutes. Sections were washed with PBS in one jet, and three more washes with PBS drops.

The labeling was revealed by incubation with 3,30-diaminobenzidine (DAB) for 15 minutes, followed by two washes with PBS, the first in a jet and the second in a drop. In the last stage, the sections were lightly counterstained with Harry's Hematoxylin (Merck) for 30 seconds and rinsed under running water.

Subsequently, the sections were incubated in 70° alcohol for 5' in an immersion bath and incubated in 95° alcohol for 5' in an immersion bath. They were incubated in Xylol for 5' and incubated again in Xylol for 10'. After draining all the remaining liquid, the slides were mounted with Canadian balm and coverslips.

For each test, negative controls were prepared in serial sections. The intensity and location of immunoreactivity with all primary antibodies used were examined throughout the content of the slide using an optical microscope. As a negative control, the primary antibody was omitted. For the image analysis study, color photomicrographs of representative areas (400x magnification) were digitally acquired. For the semiquantitative score, the images with a total of 10 images for each cut of each animal were evaluated by means of the color deconvolution tool in Image J software (NIH, USA). Pixels were categorized as previously described by Chatterjee et al.¹³, as strong positive (3+), positive (2+), weak positive (1+), and negative (0).

Flow Cytometry

Two mL of blood was collected from each animal and subsequently centrifuged at 1500 rpm for 10 min at room temperature. After centrifugation, the supernatant (serum) was pipetted and separated for analysis. The BD™ Cytometric Bead Array Mouse Inflammation Cytokine Kit (Becton

Dickinson, USA) was used for the analysis of cytokines (TNF; INF-γ; IL-6; and IL-10).

Following the manufacturer's instructions and analysis in the BD™ Accuri C6 Flow Cytometer (Becton Dickinson, USA), 10μL of each reagent was added to each sample. After this procedure, 50 μL of cytokine beads, 50 μL of each sample (serum), and 50 μL of detection reagent were placed in a 1.5 mL Eppendorf tube; the tubes were placed in the dark for 2 hours at room temperature. After two hours, 1 mL of wash buffer was added to each tube and centrifuged at 200 g and 4 °C for 5 minutes. The supernatant was carefully removed and discarded from each sample, and 300 μL of wash buffer was added to resuspend the sample.

The reading was performed manually by acquiring 10,000 events from each sample. Flow cytometry data were analyzed using the FCap 3.0 Array software (Becton Dickinson, USA), and the results were plotted in graphs of means and standard deviations of the mean.

Statistical Analysis

The data obtained were arranged in spreadsheets and analyzed using the Prism 7.0 software. The Shapiro-Wilk test was used for the normal distribution analysis. After analyzing the values in the spreadsheets, they obtained a nonnormal distribution using the Kruskal-Wallis test with Dunn's post-test.

RESULTS

The results of the main characteristics of nanoparticles are shown in Table 1. Nanoparticles presented means size about 200 nm. Several factors can influence the particle size, including formulation components (surfactant, drug characteristics) and production techniques (temperature, time, and equipment)^{14, 15}.

The polydispersion index (PDI) is a useful parameter to measure homogeneity in the distribution of diameters of all particles present in the formulation. A PDI of zero and less than 0.3 is considered ideal for a monodisperse system of

polydisperse systems¹⁶. The value found for the nanoparticles means that the formulation presented itself as a monodisperse system. The zeta potential provides the index of the magnitude of the electrostatic repulsion of particles. It is a parameter

Table 1

Characteristics of resveratrol-loaded zein/chitosan nanoparticles.

Characteristics	Results (Average \pm SD)
Particle Size (nm)	206.8 \pm 4.7
Polydispersity index (PDI)	0.172 \pm 0.16
Zeta potential (mV)	+30.00 \pm 0.33
Encapsulation Efficiency %	59.62 \pm 7.31
Characteristics	Results (Average \pm SD)
Particle Size (nm)	206.8 \pm 4.7
Polydispersity index (PDI)	0.172 \pm 0.16
Zeta potential (mV)	+30.00 \pm 0.33
Encapsulation Efficiency %	59.62 \pm 7.31

SD = Standard Deviation (n = 10)

used to determine the physical stability of colloidal systems by measuring the electrical charge on the particle surface¹⁷. The results of zeta potential suggest high colloidal stability. Finally, the encapsulation efficiency revealed that > 50% of resveratrol could interact with zein in nanoparticles.

The qualitative analysis of immunostaining for the Anti-Beta Amyloid peptide revealed light deposition of A β around the cell body of neurons in the resveratrol group (Figure 1). Moderate deposition of A β was observed in the white nanoparticles group (UN). Deposition of A β in the CA1 region around the neuron and endothelial proliferation was observed in the positive control group (PC) (Figure 1).

The quantification of beta-amyloid labeling levels was also performed. Figure 2 shows a representative image of the quantification obtained for the presence of A β in all groups. The PC and R groups showed statistically significant differences ($p < 0.005$) compared to the RN.

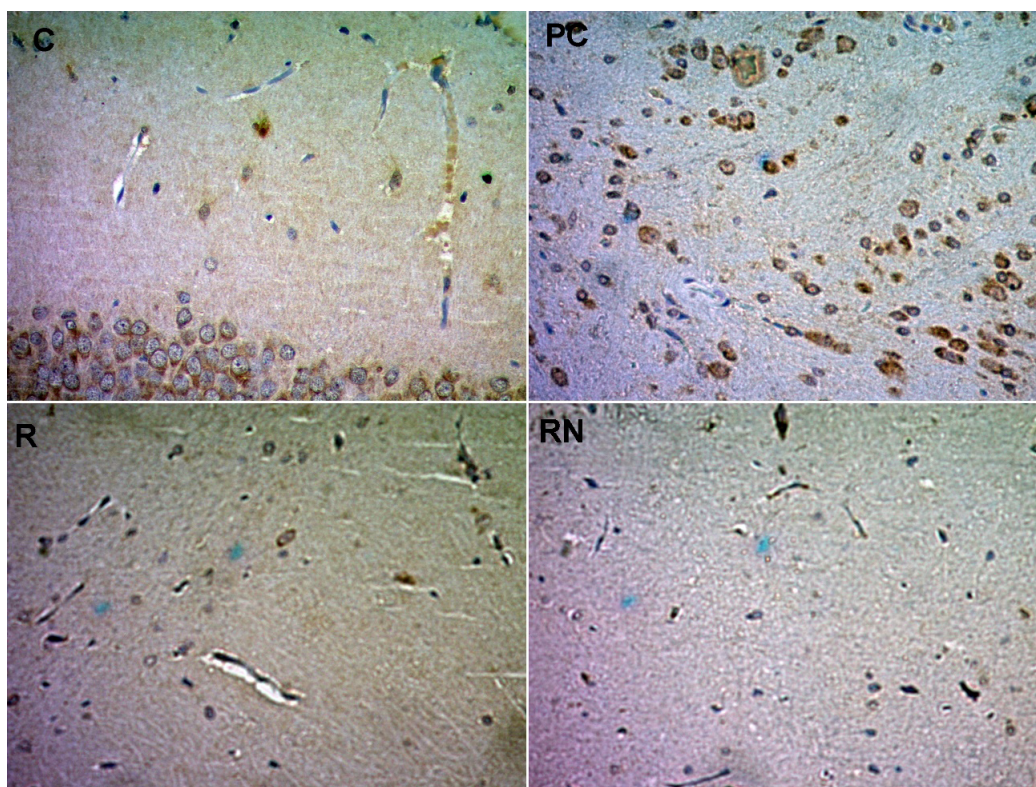


Figure 1: Immunohistochemical analysis of the Anti- β -amyloid marker (4x magnification in the left column). No morphological alterations in the RN group; deposition of Beta-amyloid in the region of CA1 was observed in the PC group; the presence of Beta-Amyloid was observed in the NB group, with the presence of Beta-Amyloid around neurons.

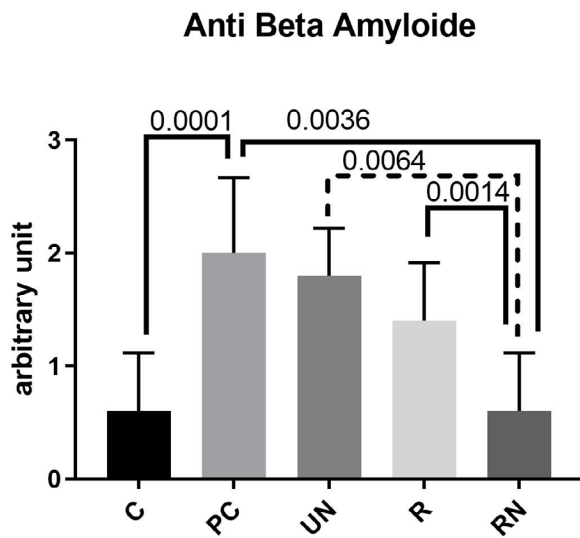


Figure 2: Quantitative analysis of the Anti-Beta-Amyloid marker in groups C and PC showed statistically significant differences ($p=0.0001$); similarly between the PC and RN groups ($p=0.0036$).

The quantification of beta-amyloid labeling levels was evaluated using Anti-Tau (Figure 3), which can be seen in the brown coloration of the axons of the hippocampus region in the C group with deposition in the region of CA1 and the supra-pyramidal lamina. Traces of Tau protein around the axons and around the cell body of neurons were also observed in the UN group. In the RN group, the Tau protein was usually deposited on the axon projection; however, noting that it is around the cell body in some neurons and does not modify the cell structure. Morphological changes in the nuclei of neurons were revealed in the group treated only with resveratrol; many of these neurons did not show a nucleus.

The quantification of the Tau protein labeling levels was observed (Figure 4). The labeling levels were similar between groups C and RN (0.4 ± 0.51 and 0.6 ± 0.51) with a coefficient of variation of 129.1% and 86.07%. The statistical analysis of quantification values showed that

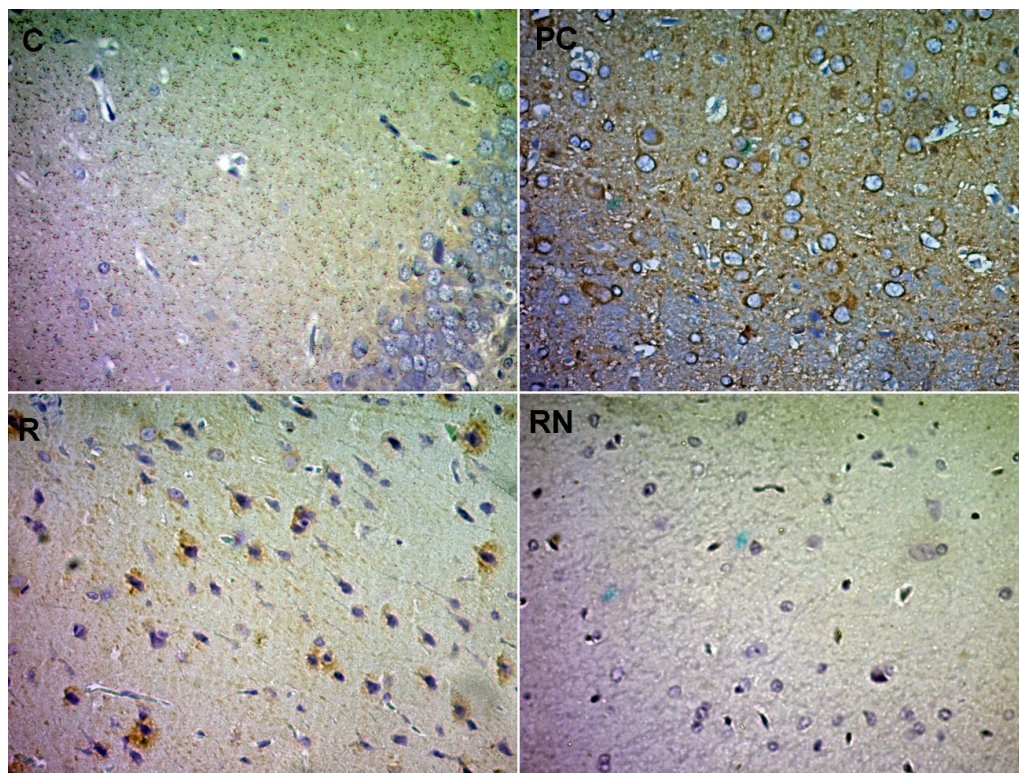


Figure 3: Protein immunohistochemical analysis of Tau (at 4x magnification on the left column and 40x on the right column). According to the demarcations in the PC, UN, R, and RN groups, the deposition can be seen as normal taurine deposition in the RN group, and different in the PC group, being noticed around the neuronal body. In the R group, modifications in the nucleus of neurons are observed.

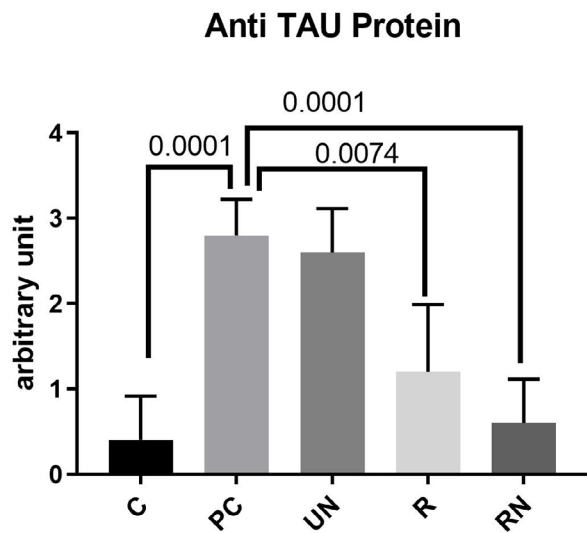


Figure 4: The quantitative analysis of Anti-Tau showed a significant difference between the C and RN groups ($p=0.0001$) and between the PC and R groups ($p=0.0074$)

there is a statistical difference between the C and RN groups ($p=0.0001$) and between the C and R groups ($p=0.0074$).

The immunohistochemistry analysis of CD68, microglia biomarkers, and defense cells (brain macrophages) is shown in Figure 5. No microglial activation was observed in group C and RN, while activation was observed in group PC. Conversely, the immunostaining in group R revealed activation of microglia, which indicates the presence of an inflammatory process.

Figure 6 shows the evaluation of microglia activation observed in groups C, UN, and R, with mean values of 1.4 ± 0.51 , 1.4 ± 0.51 , and 1 ± 0.66 , and no statistical differences between these groups. A statistically significant difference was observed between the C and RN groups ($p=0.0014$) and C and R ($p=0.0317$) groups.

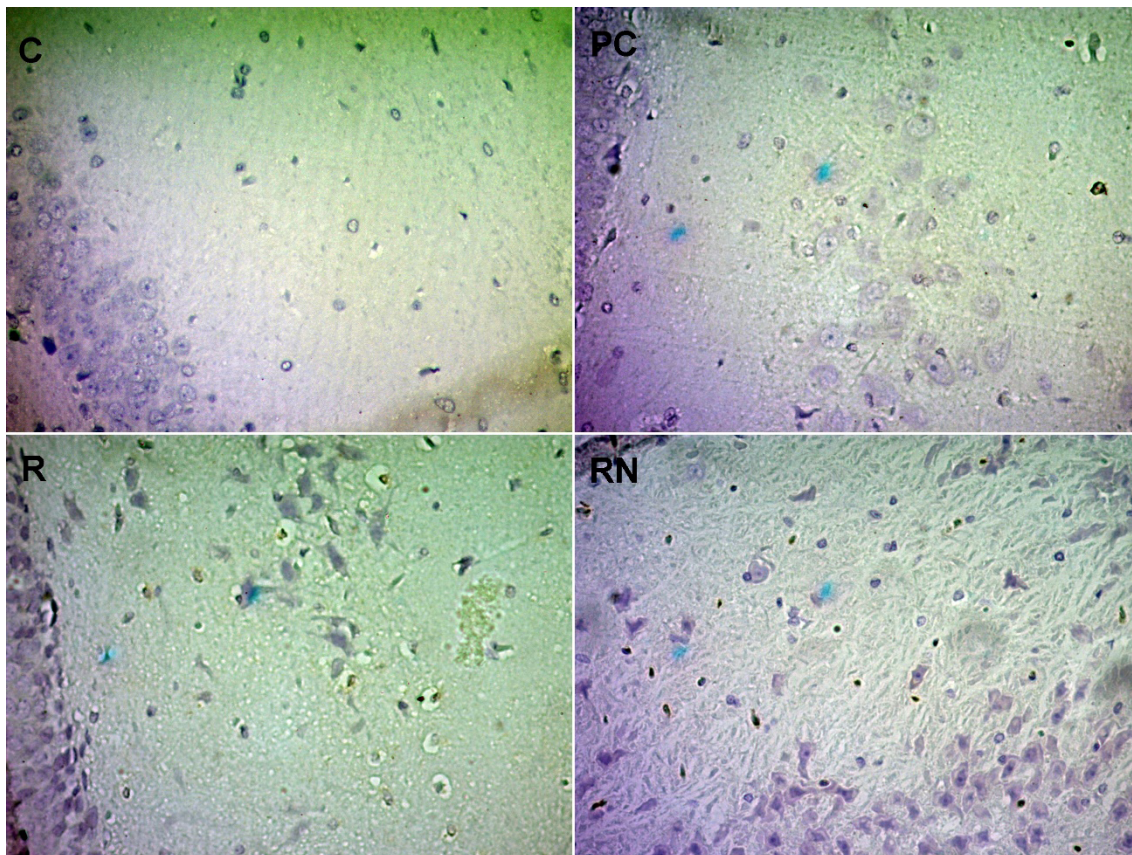


Figure 5: Immunohistochemical analysis of CD68 (with 40x magnification on the left column). No microglia activation was observed in group NR; however, an increase in microglia activation leading to a weighted inflammatory processed is observed in the UN, PC, and R groups.

The concentrations of TNF-Alpha, INF-Gamma, IL-10, and IL-6 were evaluated in the C, PC, UN, R, and RN groups. Graph 4 shows the TNF-Alpha concentration with a mean and standard deviation of 9.06 ± 2.48 in the PC group; 8.72 ± 1.97 in the R group; 5.15 ± 0.27 in the RN group, and 4.76 ± 1.08 in the C group. A significant statistical difference was observed between the C and PC

groups, C and UN groups, PC and RN group, and UN and RN groups, as shown in Figure 7.

Figure 8 shows the INF- δ observed concentration values with means and standard deviation of 3.25 ± 1.54 in the CP group, 5.31 ± 1.35 in the NB group, 6.05 ± 1.79 in the R group, and 7.50 ± 1.53 in the NR group. The statistical analysis showed no significant differences between groups. However, there was a 27% increase in R compared to C, a 15% increase in NR compared to C, and a 10% in R compared to NR; in

Anti CD68

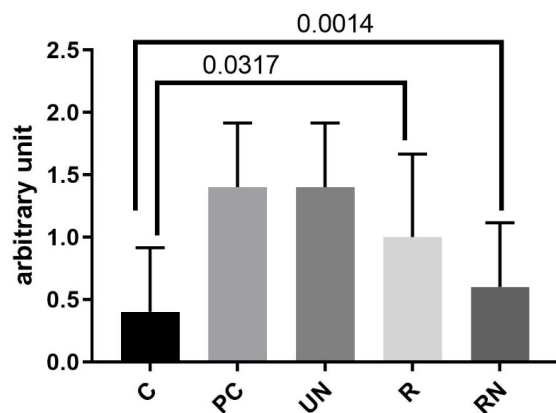


Figure 6: Quantitative analysis of CD68; a significant difference was observed between groups C and RN ($p=0.0014$) and between groups C and R ($p=0.0317$).

Interferon-Gama

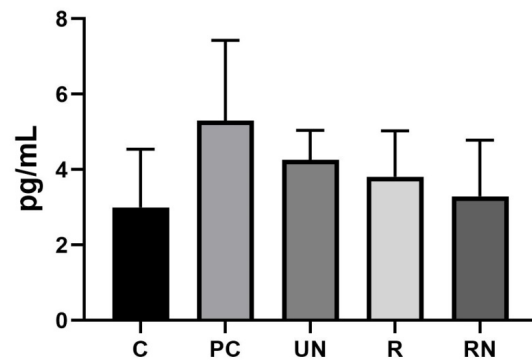


Figure 8: No statistically significant difference was observed between groups C, PC, UN, R, and RN.

TNF-Alfa

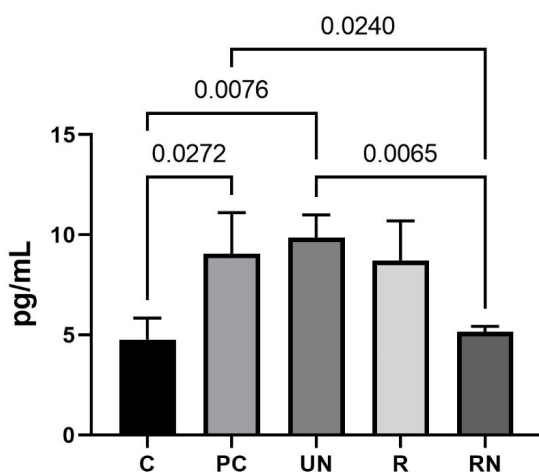


Figure 7: Representation of means between groups showing significant differences among all groups.

this perspective, the NR group was similar to the C group.

Figure 9 shows that the levels of IL-10 indicate significantly different results between groups PC and RN ($p=0.0169$). The mean values of IL-10 in the NR group were 7.50 pg/ml.

Figure 10 shows the evaluated levels of IL-6 with a significant difference between the RN and R groups ($p=0.0234$). The mean values of IL-6 in the PC, UN, R, and RN groups were 5.27 pg/ml, 4.71 pg/ml, 5.09 pg/ml, and 3.23 pg/ml, respectively.

DISCUSSION

AD involves several complications and alterations that may be irreversible, as reported in the study by Beckes *et al.*¹⁸. Hence, the exploration of

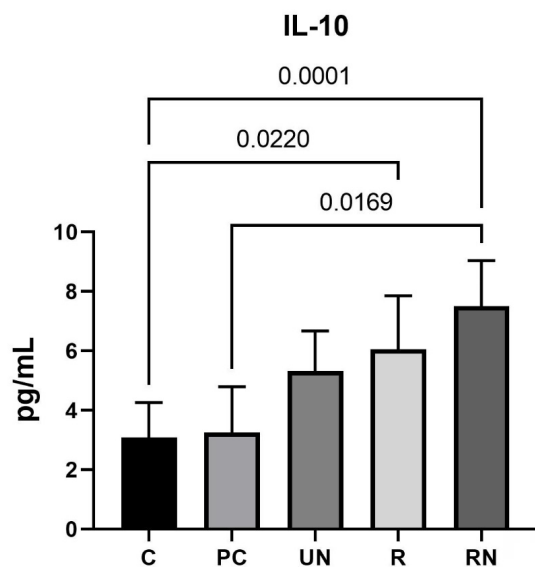


Figure 9: Representation of the means of comparison between the RN and R groups.

interactions and interrelationships that can promote and recover the health of the individual who is in this situation is relevant. ILHA *et al.*¹⁹ highlighted the importance of using artifacts to promote improvement in quality of life, socialization, acceptance, and capacity for activities of daily living for AD patients.

AD is a degenerative disease that causes progressive damage to brain tissue, which leads to loss of synapses, damage, and neuronal death. Silva *et al.*²⁰ believe in the consensus knowledge of an accumulation of amyloid plaques in these patients' brains, which is in agreement with the results of the present study, showing the accumulation of amyloid plaques in the untreated groups and significant differences in the group treated with resveratrol nanoparticles.

The amyloid precursor protein (PPA) is a membrane protein with the main function of allowing the plasticity of synapses, acting in the process of building memory, reasoning, and thinking. However, PPA can undergo cleavage processes by the β -secretase enzyme and the γ -secretase enzyme (5).

In this study, A β 1-42 fragments were infused in the hippocampal region of CA1. A greater formation of A β was observed in the NB and CP

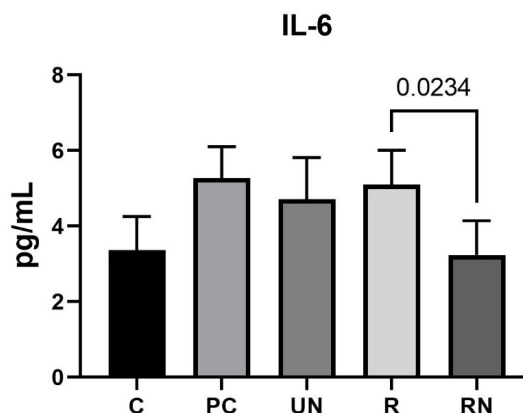


Figure 10: Representation of the mean between the R and RN groups.

groups together with neuronal death. If the peptide accumulates in the extracellular region of the diseased brain, it ends up forming senile plaques, leading to neuronal loss and brain atrophy, which can be found in these groups (NB and CP).

Studies by Capirala *et al.*²¹ and Zhong¹⁰ reported that resveratrol significantly reduces the production of pro-inflammatory cytokines (IL-1 and TNF) induced by lipopolysaccharide (LPS) or A β in microglia.

In this study, it was possible to observe that the deposition of A β in the R group occurred mildly while no deposition or microglia activation was observed in the NR group. These findings are similar to those described by Capirala *et al.*²¹ and Zhong¹⁰.

Hambardzumyan *et al.*²² reported that in addition to the significant roles of resveratrol as an antioxidant and anti-inflammatory, there is evidence to suggest that it also facilitates the non-amyloidogenic breakdown of the amyloid precursor protein (PPA), which may have resulted in the observed non-deposition of A β in our study.

According to Mehrabadi and Sadr²³, microglia activation releases pro-inflammatory cytokines such as IL1 β , IFN- δ , and TNF- α . Thus, in the present study, the production of TNF- α was lower in the RN group than in the PC group.

Many studies report the activation of microglia and proinflammatory cytokines in AD as important in neuroinflammation and neurodegeneration. Our analysis of IL10 shows that

there was a significant statistical difference between the PC and RN groups, demonstrating that the nanoparticles containing resveratrol can be effective in combating neuroinflammation and neurodegeneration.

The studies of Salem *et al.*²⁴ using trans-ferosomal nanoemulsions with resveratrol to evaluate the brain targeting system on memory showed permeation results of up to 81.29% ± 2.64%, which they claim as a great option for treatment. However, in this study, the quantification of nanoparticles containing resveratrol in the brains of animals was not conducted. Nevertheless, our analyses show that the nanoparticles containing resveratrol achieved encephalic reach, hence preventing the appearance of senile plaque and microglia activation.

Several mechanisms have been described as involved in the causation of AD, such as genetic, epigenetic, metabolic factors, inflammatory reactions, mitochondrial pathogenic cascade, oxidative stress, plasma and brain proteins, brain-derived neurotrophic factor (brain-derived neurotrophic factor-BDNF), estrogen deficiencies, and environmental factors.

CONCLUSION

The present study reveals the benefits of resveratrol nanoparticles in the inhibition of Beta-Amyloid deposition in neuroinflammation processes in an experimental model induced by Beta Amyloid1-42.

LIMITATION OF THE STUDY

Because the present study was carried out in a public teaching institution, the lack of financial support resulted in difficulties in the performance of the studies in some of the research sectors.

HUMAN AND ANIMAL RIGHTS

Animals were used for the studies that are the basis of this research (protocol number 031/2019).

REFERENCES

1. Pandey G, Ramakrishnan V. Invasive and non-invasive therapies for Alzheimer's disease and other amyloidosis. *Biophys. Rev.* 2020; 12:1175-1186. <https://doi.org/10.1007/s12551-020-00752-y>
2. Falco A, Cukierman DS, Hauser-Davis RA e Rey NA. Doença De Alzheimer: Hipóteses Etiológicas E Perspectivas De Tratamento. *Quim. Nova.* 2016; 39(1): 63-80.
3. Shengquan H, Yanfang X, Yubo F, Shinghung M, Jiajun W, Jing T, Yuanping P, Rongbiao P, Karl WT, Fufeng L, Zhixiu L, Yifan H. Significant combination of A β aggregation inhibitory and neuroprotective properties in silico, in vitro and in vivo by bis(propyl)-cognitin, a multifunctional anti-Alzheimer's agent. *European J. of Pharmacol.* 2020; 876, 1-10.
4. Sawda, C, Moussa, C, Turner, RS. Resveratrol for Alzheimer's disease. *Anais da Academia de Ciências de Nova York.* 2017; 1403(1):142-149.
5. Silva LR, Vianna CMM, Mosegui GBG, Peregrino AAF, Marinho V, Laks J. Cost-effectiveness analysis of the treatment of mild and moderate Alzheimer's disease in Brazil. *Braz. J. Psychiatr.* 2019. 41(3): 218-224.
6. Ministério da Saúde. Protocolo Clínico e Diretrizes Terapêuticas- Doença de Alzheimer. PORTARIA CONJUNTA Nº 13. 2017.
7. Piovesana MCFS, Garcia FR, Carrasco KG, Tognola WA. Reassessment of the dementia diagnosis of Alzheimer's disease in patients enrolled on the cholinesterase inhibitors dispensation program. *Dement. Neuropsychol.* 2012; 6 (4): 270-275.
8. Cheng, G., Xu P, Zhang M, Chen J, Sheng R, Ma Y. Resveratrol-maltol hybrids as multi-target-directed agents for Alzheimer's disease. *Bioorganic & Med. Chem.* 2018; 26(22):5759-5765.
9. Jeřábek J, Uliassi E, Guidotti L, Korabecny J, Soukup O, Sepsova V, Hrabínova M, Kuca K, Bartolini M, Peña Altamira MA, Petralla S, Monti B, Roberti M, Bolognesi M L. Tacrine-resveratrol fused hybrids as multi-target-directed ligands against Alzheimer's disease, *European J. of Med. Chem.* 2017; 127:250-262. <https://doi.org/10.1016/j.ejmech.2016.12.048>
10. Zhong Q, Jim M. Zein nanoparticles produced by liquid-liquid dispersion. *Food Hydrocoll.* 2009; 23 (8): 2380-2387.
11. Pauluk D, Padilha AK, Khalil NM, Rubiana MM. Chitosan-coated zein nanoparticles for oral delivery of resveratrol: Formation, characterization, stability, mucoadhesive properties and antioxidant activity. *Food Hydrocoll.* 2019; 94:411-417.
12. Panis LI, Geus BD, Vandenbulcke G, Willems H, Degraeuwe B, Bleux N, Mishra V, Thomas I, Meeusen R. Exposure to particulate matter in traffic: A comparison of cyclists and car passengers. *Atmospheric Environment.* 2010; 44(10):2263-2270.

13. Chatterjee A, Zakian S, Hu X, Singleton MR. Structural insights into the regulation of cohesion establishment by Wpl1. *The EMBO J.* 2013; 32(5):677-687.
14. Marcato PD. Preparação, caracterização e aplicações em fármacos e cosméticos de nanopartículas lipídicas sólidas. *Revista Eletrônica de Farmácia.* 2009; 6(2):1-37.
15. Maraicar KSH, Thirumoorthy N. Design and characterization of solid lipid nanoparticles by solvent evaporation method followed by homogenization. *Int. J. of Biopharm.* 2014; 014 5(3): 190-196.
16. Jawahar N, Meyyanathan SN, Reddy G, Sood S. Solid lipid nanoparticles for oral delivery of poorly soluble drugs. *J. of Pharm. Sci. & Res.* 2012; 4(7):1848-1855.
17. Surender V, Deepika M. Solid lipid nanoparticles: a comprehensive review. *J. of Chem. and Pharm. Res.* 2016; 8(8):102-114.
18. Beckes DS, Zamberlan C, Colomé J, Souza MT, Marchiori MT, Erdann AL, Salazar-Maya AM. Interatividade sistêmica entre os conceitos interdependentes de cuidado de enfermagem. *Aquichan.* 2016; 16 (1):23-31.
19. Ilha S, Santos SSC, Backes DS, Barros E JL, Pelzer MT, Gautério-Abreu DP. Gerontotecnologias utilizadas pelos familiares/ cuidadores de idosos com Alzheimer: contribuição ao cuidado complexo. *Texto Contexto Enfermagem.* 2018; 27(4):1=16. <https://doi.org/10.1590/0104-07072018005210017>
20. Silva TU, Freitas LV, Rey NA, Machado SP. Estudo Teórico de potenciais agentes para o tratamento da doença de Alzheimer derivados da 8- Hidroxiquinolina com substituintes do tipo N-ACIL—hidrazona. *Quim. Nova.* 2018; 41(10):1132-1139.
21. Capiralla H, Vingtdoux V, Zhao H, Sankowski R, Al-Abed Y, Davies P, Marambaud P. Resveratrol mitigates lipopolysaccharide- and A-mediated microglial inflammation by inhibiting the TLR4/NF-kappaB/STAT signaling cascade. *J. Neurochem.* 2012; 120:461-472.
22. Hambardzumyan D, Gutimann DH, Kettenman H. The role of microglia and macrophages in glioma maintenance and progression. *Nat. Neurosci.* 2015; 19(1):20.
23. Mehrabadi S, Sadr SS. Assessment of Probiotics Mixture on Memory Function, Inflammation Markers, and Oxidative Stress in an Alzheimer's Disease Model of Rats. *Iran Biomed. J.* 2020; 24(4):220-228. doi:10.29252/ibj.24.4.220
24. Salem HF, Khaershoum MR, Abou-Taleb HA, Naguig DM. Brain targeting of resveratrol through intranasal lipid vesicles labelled with gold nanoparticles: *in vivo* evaluation and bioaccumulation investigation using computed tomography and histopathological examination. *J. of Drug Targeting.* 2019; 27(10):1127-1134.

Authors' contribution:

Mariane Maria Silveira Vieira de Lima: conceptualization, methodology, writing

Flávio Klinpovous Kerppers: methodology, data curation

Ketllin Bragnholo: methodology, data curation

Luiza Ferreira Cunha: methodology, data curation

Maiara Fonseca: methodology, data curation

Tatiane Budniak Mazur: methodology, data curation

Maria Elvira Ribeiro Cordeiro: methodology, data curation

Christiane Schneider Machado: methodology

Rubiana Mara Mainardes: methodology

Afonso Shiguemi Inoue Salgado: supervision and review

André Alexandre Pezzini: supervision and review

Ana Carolina Dorigoni Bini: supervision and review

Ivo Ilvan kerppers: supervision and review

Consent for publication

Not applicable.

Conflict Of Interest

The authors declare no conflicts of interest, financial or otherwise.

Funding

This research did not receive any specific grant from funding agencies in the public, commercial, or not-for-profit sectors.

This manuscript was translated and reviewed by a professional science translator/editor to improve readability. Nice Shindo, Ph.D. (niceshindo@gmail.com).

Corresponding Author:
Maria Elvira Ribeiro Cordeiro
mariaelvirar.99@gmail.com

Editor:
Prof. Dr. Paulo Henrique Manso

Received: jan 31, 2023
Approved: may 31, 2023
